VI International Conference on Computational Methods in Marine Engineering
MARINE 2015
F. Salvatore, R. Broglia and R. Muscari (Eds)

TURBULENT MARINE BOTTOM BOUNDARY LAYER BY $\overline{V'^2}$-F TURBULENCE MODEL

H. SMAOUI[1,2], S. KAIDI[1,2] and N. HUYBRECHTS[1,2]

[1]CEREMA-DTecEMF
134, rue de Beauvais - CS 60039
60280 Margny-lès-Compiègne, France
e-mail: hassan.smaoui@cerema.fr and sami.kaidi@cerema.fr

and

[2] Sorbonne universités, Université de Technologie de Compiègne, laboratoire Roberval
CS 60319, 60203 Compiègne cedex, France
e-mail: hassan.smaoui@utc.fr and sami.kaidi@utc.fr

Key words: hydrodynamics, turbulence, boundary layer, wave, tide, sediment transport

Abstract. In this work, we propose to implement the $\overline{v'^2} - f$ turbulence model rarely used in the marine environment to study the marine bottom boundary layer (MBBL). This model will complete the series of the turbulence models already implemented in the operational model 1DV-MoSeTT (1D Vertical Model of Sediment Transport and Turbulence) developed for the MBBL dynamics analysis .
To show the performance of $\overline{v'^2} - f$ turbulence model first, we give a comparison between this model and $q^2 - q^2\ell$ model. This comparison is based in various laboratory data proposed in the literature and widely used by the scientific community. Second, and in comparison with *in-situ* suspended sediment transport measurements, we examine the impact of the $\overline{v'^2} - f$ and the $q^2 - q^2\ell$ turbulence models on the quantification of flux sediment at the bottom and on the estimation of the vertical profile of the suspended particle matter (SPM).

1 INTRODUCTION

The presence of suspended sediment quantities in coastal areas raises difficult problems with expensive costs generation for developments, maintenance and preservation of navigation channels (dredging). Control and understanding of interactions at the water-sediment interface turn out to be extremely complex because of the presence of numerous processes with very different space and time scales. In the other hand, coastal and estuarine circulation reached very high Reynolds number what characterizes fundamentally turbulent flows. Therefore, a good estimation of these flows requires good turbulence

modeling (choice of suitable turbulence model). Also, it should be noted that turbulence is a key parameter for the quantification of sediment flux at the sediment-water interface and in particular in a marine bottom boundary layer.
Many simulations of fluid flow show that the standard $k-\varepsilon$ model with wall laws fail to predict correctly the friction at the walls. Indeed, the turbulent variables are resolved only from the inertial layer to the surface and the connection to the wall is achieved by the expression of the logarithmic law valid in the inertial sublayer. To overcome this shortcoming, several turbulence models were developed for flow configurations with low Reynolds number (LRe). We cite per example the $k-\varepsilon-LRe$ model due to Chien [1], the $k-\omega$ model due to Wilcox [2] and the SST $k-\omega$ model due to Menter [3]. Note that these models have the disadvantage to not include neither the turbulence anisotropy near the wall, nor the non-local effects induced by pression deformation. In order to improve the modeling of turbulence on these two aspects, Durbin [4] proposed the $\overline{v'^2}-f$ model that quickly became popular by its ability to estimate with good accuracy of the turbulence of increasingly complex flow configurations.
The purpose of this work is to evaluate the performance of the $\overline{v'^2}-f$ model applied to a MBBL generated by a purely oscillatory pressure gradient (tide or wave). The $\overline{v'^2}-f$ model will be implemented in the operational computer code 1DV-MoSeTT in which the turbulent variables are estimated by the $q^2-q^2\ell$ turbulence model due to Mellor and Yamada [5]. At first, the numerical results obtained by the $\overline{v'^2}-f$ model will be compared to both measurement obtained in laboratory by Sleath [6]to study a purely oscillatory MBBL and the results obtained by the $q^2-q^2\ell$ model initially implemented in the 1DV-MoSeTT code. At the second time, the $\overline{v'^2}-f$ model will be tested on the ability to reproduce the SPM peaks observed *in-situ* in the Eastern part of the English Channel. The instruments used to obtain these measurements were deployed from 21 to 24 September 1996 within the framework of the *MAST3* programme *PRe-Operational Modelling In the Seas of Europe* (*PROMISE*) funded by the Commission of the European Union.

2 PRESENTATION OF THE MATHEMATICAL MODEL

2.1 Assumptions

The 1DV model used in this study is based on the 3D version of the free surface flow models, but wherein all horizontal gradients were neglected except the pressure gradient. It assumed negligible depth variations associated with tidal waves, and assumed flow was unstratified. The 1D model consists of two equations of momentum equation, two equations for the turbulent variables and a transport equation of the SPM. Note that the 1DV model was originally developed for application to the Eastern part of the English Channel. This zone is characterized by an intensely turbulent flow dominated by the $M2$ tidal wave of frequency $\omega = 2.23 \times 10^{-5}$. In the same way the Coriolis parameter at this zone is $f = 11.27 \times 10^{-5}$ ($f > \omega$). Consequently, effects of the earth's rotation should be included in the model equations.

2.2 Governing equations

Based on the above assumptions, the linearized Reynolds-averaged governing equations for the tidal flow cartesian coordinate system consists in the following set of equations

$$\frac{\partial u}{\partial t} = -\frac{1}{\rho}\frac{\partial p}{\partial x} + fv + \frac{\partial}{\partial z}\left[(\nu + \nu_t)\frac{\partial u}{\partial z}\right] \tag{1}$$

$$\frac{\partial v}{\partial t} = -\frac{1}{\rho}\frac{\partial p}{\partial y} - fu + \frac{\partial}{\partial z}\left[(\nu + \nu_t)\frac{\partial v}{\partial z}\right] \tag{2}$$

$$\frac{\partial q^2}{\partial t} = \frac{\partial}{\partial z}\left(\nu_{tq}\frac{\partial q^2}{\partial z}\right) + 2\nu_t\left[\left(\frac{\partial u}{\partial z}\right)^2 + \left(\frac{\partial v}{\partial z}\right)^2\right] - \frac{2q^3}{B_1\ell} \tag{3}$$

$$\frac{\partial q^2\ell}{\partial t} = \frac{\partial}{\partial z}\left(\nu_{tq}\frac{\partial q^2\ell}{\partial z}\right) + E_1\ell\nu_t\left[\left(\frac{\partial u}{\partial z}\right)^2 + \left(\frac{\partial v}{\partial z}\right)^2\right] - \frac{q^3\tilde{w}}{B_1} \tag{4}$$

$$\frac{\partial c}{\partial t} = w_s\frac{\partial c}{\partial z} + \frac{\partial}{\partial z}\left[(\gamma + \gamma_t)\frac{\partial c}{\partial z}\right] \tag{5}$$

with x extending eastward, y extending northward, and z extending upward positively from the seabed. In the above equations t the time, u and v are the x, y velocity components, ρ the water density, p denotes the pressure, f the Coriolis parameter, ν the molecular viscosity, and ν_t represents the turbulent eddy viscosity, $k = q^2/2$ is the TKE (turbulent kinetic energy), ℓ the turbulence macroscale length, ν_{tq} the turbulent diffusivity of TKE, $\tilde{w}$ is the wall function, B_1, E_1 are empirical constants (Table 2), c the concentration of SPM, γ and γ_t are the molecular and the turbulent diffusivity of SPM and w_s is the settling velocity given by

$$w_s = \begin{cases} \dfrac{gd_{50}^2(s-1)}{18\nu} & \text{if } d_{50} < 63\mu m \\ \dfrac{-3\nu + \sqrt{9\nu^2 + gd_{50}^2(s-1)(\alpha_1 + \alpha_2 d_{50})}}{\beta_1 + \beta_2 d_{50}} & \text{if } d_{50} \geq 63\mu m \end{cases} \tag{6}$$

Where g is the acceleration of gravity, d_{50} is the median diameter of the sediments, $s = \rho_s/\rho$, ρ_s is the density of the sediments and $\alpha_1, \alpha_2, \beta_1, \beta_2$ are empirical constants (Table 1).

α_1	α_2	β_1	β_2
3.8691×10^{-5}	2.4801×10^{-2}	1.1607×10^{-4}	7.4405×10^{-2}

Table 1: Empirical constants used to compute the settling velocity w_s

To close the system of equations (1, 2, 3, 4, 5), the turbulent viscosity ν_t and diffusivities (ν_{tk}, γ_t) must be determined from TKE k, the mixing macroscale length ℓ and same stability functions S_m, S_k and S_h as :

$$\nu_t = \ell\sqrt{k}S_m \qquad , \qquad \nu_{tk} = \ell\sqrt{k}S_k \qquad , \qquad \gamma_t = \frac{S_h}{S_m}\nu_t \tag{7}$$

S_q is an empirical constat, S_m and S_h are the stability functions, which are simple algebraic functions of local stratification (for details, see , [5]).

B_1	E_1	S_h	S_k	S_m
16.6	1.80	0.49	0.20	0.39

Table 2: Closure empirical constants of $q^2 - q^2\ell$ turbulence model

2.3 Boundary conditions

The governing set of partial differential equations PDEs (1-5) must be solved based on boundary conditions at the seabed and the free surface. This first limit of the bottom boundary layer is designed by z_0 (bed roughness), defined as the height above seabed at which fluid velocity cancels out.
The bed roughness is an important parameter to calculate the bed shear stress and its related quantities near the bed. The parameter $z_0 = k_b/30$ depends on the local bottom roughness k_b (roughness height designed also the equivalent Nikuradse roughness). For the flat bed with little sediment motion the roughness height is determined by the sediment grain on the bed. For example, based on steady flow flume experiments Van Rijn [7] found that roughness height is mainly determined by the largest grains. Therefore he proposed $k_b = 3d_{90}$ for oscillatory flow.

2.3.1 At the bottom

At the bottom, a non-slip condition is assumed for the velocities ($u(z_0) = v(z_0) = 0$). Moreover, if we assume the equilibrium between the production and the dissipation of the TKE, the logarithmic profil of the velocity (u, v) and a linear mixing length, the following conditions can be imposed for k and ℓ

$$k(z_0) = \frac{B_1^{2/3}}{2}u_*^2 \qquad , \qquad \ell(z_0) = \kappa z_0 \tag{8}$$

here u_* is the bottom friction velocity, and κ is the Von Karmàn constant ($\kappa = 0.41$).

For the SPM equation (5), the Neumann condition can be applied when expressing seabed conditions. Therefore, the bottom boundary condition for c specified net mass flux

through water sediment interface. This flux is the difference between downward advection caused by particle settling (deposition rate D) and upward entrainment of sediment from the seabed (erosion rate E).

$$w_s c - \gamma_t \frac{\partial c}{\partial z} = D - E \tag{9}$$

The deposition rate D is considered proportional to the SPM concentration close to the bed with the settling velocity w_s acting as a proportionality factor ($D = w_s c(z_0)$). In addition, the erosion rate E is computed by the equation (10) given in the equilibrium condition by [8]:

$$E = w_s c_b \frac{\gamma_0 S}{1 + \gamma_0 S} \tag{10}$$

where c_b is the volume concentration of the sediment ($c_b = 0.65$ for non-cohesive sediment), γ_0 is an empirical constant for the sediment re-suspension and S is the non-dimensional shear stress excess given by:

$$S = \frac{\tau_b - \tau_{th}}{\tau_{th}} \tag{11}$$

$\tau_b = \rho u_*^2$ is the shear stress at the bottom and τ_{th} the critical threshold for erosion.

2.3.2 At the sea surface

At the sea surface $z = H$ and in the absence of wind, the shear stress, turbulent kinetic energy k and turbulence macro-scale ℓ are assumed to have a vertical gradient of zero, thus

$$\frac{\partial \overline{u}}{\partial z} = 0, \qquad \frac{\partial \overline{v}}{\partial z} = 0 \tag{12}$$

$$\frac{\partial k}{\partial z} = 0, \qquad \frac{\partial k\ell}{\partial z} = 0 \tag{13}$$

The surface boundary condition for the SPM c is

$$w_s c - \gamma_t \frac{\partial c}{\partial z} = 0 \tag{14}$$

2.4 Turbulence model $\overline{v'^2} - f$

Turbulence models based on $k-\varepsilon$ have been developed for parallel flows to the wall. For some applications involving situations where the flow is not parallel to the wall (fluid/wall impact zone), these models are inaccurate. In particular, an overestimation of turbulence is often predicted in these impact areas, with dramatic consequences for the prediction of the mixture phenomena. For example, the standard $k - \varepsilon$ model overestimates of 100% the heat transfer in a jet impact on a heated wall. To avoid this type of behavior, Durbin [9] was developed the $\overline{v'^2} - f$ model. This model can be considered as an intermediary between the turbulent viscosity concept and the turbulence second order modeling.

It retains the assumption of turbulent viscosity, essential to maintain a high numerical stability. It allows modeling both the non-local properties (anisotropy) of turbulence at fluid-wall interface as well as the pressure-strain correlations (without using the two-points correlations approach). To predict the anisotropy of parietal turbulence, the $\overline{v'^2}-f$ model introduces a new turbulent velocity scale called $\overline{v'^2}$ independently of the TKE k. Note that in the second-order turbulence modeling, the TKE, is not able to model correctly the transport damping by turbulence near the solid walls. To correct this issue, the $\overline{v'^2}-f$ model proposes an evaluation of the turbulent viscosity based on the turbulent variable $\overline{v'^2}$ (instead of k) and a new timescale noted $\mathcal{T}$.
Note also that $\overline{v'^2}-f$ turbulence model introduces a new dimensionless quantity (noted f) which describes the turbulente energy redistribution. This quantity governed by an elliptic operator evaluates the pressure-strain correlations while avoiding the use of two-points correlations concept which is not appropriate in inhomogeneous turbulence. All these improvements will be obtain by the $\overline{v'^2}-f$ model by solving additional PDEs. Thus, the $\overline{v'^2}-f$ model consists of four transport equations for four variables k, ε, $\overline{v'^2}$ and f given by:

$$\frac{\partial k}{\partial t}=\frac{\partial}{\partial z}\left[\left(\nu_m+\frac{\nu_t}{\sigma_k}\right)\frac{\partial k}{\partial z}\right]+P_k-\varepsilon \tag{15}$$

$$\frac{\partial \varepsilon}{\partial t}=\frac{\partial}{\partial z}\left[\left(\nu_m+\frac{\nu_t}{\sigma_\varepsilon}\right)\frac{\partial \varepsilon}{\partial z}\right]+\frac{C'_{\varepsilon 1}P_k-C_{\varepsilon 2}\varepsilon}{\mathcal{T}} \tag{16}$$

$$\frac{\partial \overline{v'^2}}{\partial t}=\frac{\partial}{\partial z}\left[\left(\nu_m+\frac{\nu_t}{\sigma_v}\right)\frac{\partial \overline{v'^2}}{\partial z}\right]+kf-\frac{\overline{v'^2}}{k}\varepsilon \tag{17}$$

$$L^2\frac{\partial^2 f}{\partial z^2}-f=\frac{C_1-1}{\mathcal{T}}\left(\frac{\overline{v'^2}}{k}-\frac{2}{3}\right)-C_2\frac{P_k}{\mathcal{T}}-5\frac{\overline{v'^2}}{k\mathcal{T}} \tag{18}$$

Where P_k is the TKE production term , $\mathcal{T}$ is a characteristic time scale of turbulence and L is a characteristic length scale of turbulence. These quantities are given respectively by:

$$P_k=\nu_t\left(\frac{\partial u}{\partial z}\right)^2 \quad , \quad \mathcal{T}=max\left(\frac{k}{\varepsilon},6\sqrt{\frac{\nu_m}{\varepsilon}}\right) \quad , \quad L=C_L max\left(\frac{k^{3/2}}{\varepsilon},C_\eta\frac{\nu_m^{3/4}}{\varepsilon^{1/4}}\right)$$

For $\overline{v'^2}-f$ turbulence model, the constant $C_{\varepsilon 1}$ of the standard $k-\varepsilon$ model was modified to take the value $C'_{\varepsilon 1}=1.4\left(1+C_{\varepsilon d}\sqrt{\frac{k}{\overline{v'^2}}}\right)$.

Now the turbulent viscosity ν_t is expressed with the new turbulent velocity scale $\overline{v'^2}$ as:

$$\nu_t=C_\mu\overline{v'^2}\mathcal{T} \tag{19}$$

The expressions of parameters $\mathcal{T}$ and L were derived from the realizability condition of $\overline{v'^2}-f$ in order to avoid non-physical solutions (i.e., $\overline{v'^2}<0$ and $\overline{v'^2}>2k$).

Table (3) summarizes the values of all empirical constants appearing in the $\overline{v'^2} - f$ equations model.

C_1	C_2	C_L	C_η	C_μ	$C_{\varepsilon d}$	$C_{\varepsilon 2}$	σ_k	σ_ε	σ_v
0.4	0.3	0.3	85	0.19	0.045	1.9	1.0	1.3	1.0

Table 3: Empirical constants of the $\overline{v'^2} - f$ model

To solve the set of equations (15 to 18) value of each variable must be given at the boundary of the water column (bottom and surface). Durbin [9] showed that near the bottom ($z = z_0$) k, ε, $\overline{v'^2}$ and f behave asymptotically as

$$k \sim O(z^2) \quad , \quad \overline{v'^2} \sim O(z^4) \quad , \quad \varepsilon \sim O(1) \quad , \quad f \sim O(1)$$

In other words, at the bottom ($z \longrightarrow z_0$) one can impose $k(z_0) = \overline{v'^2}(z_0) = 0$). Moreover, if we perform an asymptotic analysis of equations (15) and (17) near the bottom, we get:

$$\varepsilon \longrightarrow \frac{2\nu k}{z^2} \quad , \quad kf \longrightarrow -5\frac{\overline{v'^2}\varepsilon}{k} \quad \text{or } f \longrightarrow -20\frac{\nu^2\overline{v'^2}}{\varepsilon z^4}$$

Finally, At the free surface located at $z = z_h$, we impose the condition of symmetry for the variables k, ε, $\overline{v'^2}$ et f ,i.e., $\left(\frac{\partial k}{\partial z} = \frac{\partial \varepsilon}{\partial z} = \frac{\partial \overline{v'^2}}{\partial z} = \frac{\partial f}{\partial z} = 0\right)$. However, for velocity u we impose either a condition of symmetry condition, or type of Dirichlet condition $u = U_h$.

As mentioned earlier, the aim of this paper is to integrate the $\overline{v'^2} - f$ turbulence model in the computer code 1DV-MoSeTT. This involves replacing the equations of q^2 and $q^2\ell$ by a set of equations defining the $\overline{v'^2} - f$ model. Thus, the final system of PDEs solved in this paper consists of sets equations (1, 2, 5, 15, 16, 17, 18) and their associated boundary conditions.

2.5 Numerical solution

The flow modelled in this study is the bottom boundary layer flow type. The variables of this type of flow are characterized by large variations in the vicinities of the bottom of the domain. To reproduce numerically these variations, we used a variable mesh size by splitting the column water into three layers (bottom, intermediate and surface layer). The bottom layers were meshed very fine (about one millimeter). To limit interpolation procedures during the computation , the mean variables (u, v and c) and the turbulent variables (k, ε, $\overline{v'^2}$, ν_t, γ_t) were calculated on two staggered grids.
All PDEs of the numerical model with their boundary conditions were discretized by the finite volume method in space and finite differences in time. The spatial partial derivatives were approximated by a centered scheme except the convective term of equation (5). The implicit Euler scheme was adopted for the time derivatives of all model equations. Note

that the discretization of equations has led to solve a tri-diagonal linear system by the Thoma's algorithm (TDMA: tri-diagonal Matrix Algorithm).

3 COMPARISON OF TURBULENCE MODELS $\overline{v'^2} - f$ AND $q^2 - q^2\ell$

To test the performances of the $\overline{v'^2} - f$ and $q^2 - q^2\ell$ turbulence models, we briefly compare the results of these two models to those measured by Sleath [6]. These measurements were performed for a flow generated by a wave in a flat and horizontal bottom boundary layer (BBL) of roughness $z_0 = k_b/30$ which propagates in the x-axis direction. Coriolis effects are not included. With these assumptions, the hydrodynamical equations will be reduce to

$$\frac{\partial u}{\partial t} = -\frac{1}{\rho}\frac{\partial p}{\partial x} + \frac{\partial}{\partial z}\left[(\nu + \nu_t)\frac{\partial u}{\partial z}\right] \tag{20}$$

The horizontal movement of the wave can be represented by a oscillatory flow outside the boundary layer. Since the wave BBL thickness is very "small", it can be assumed that the wave pressure gradient in the inner boundary layer is independent of z and it is equal to the external wave pressure gradient [10]. Thus

$$-\frac{1}{\rho}\frac{\partial p}{\partial x} = \frac{\partial U_h}{\partial t} = \widehat{U}_h \omega_h \cos(\omega t) \tag{21}$$

where U_h is the wave velocity at the top of the boundary layer, the $\widehat{U}_h$ it's amplitude and $\omega_h = 2\pi/T_h$ is the wave angular frequency. Table (4) summarizes the main parameters of these measurements in witch $\widehat{a}_h$ is the orbital amplitude of the wave ($\widehat{a}_h = \widehat{U}_h/\omega_h$) and z_h is the top of the boundary layer.

$\widehat{U}_h(cm/s)$	$T_h(s)$	$\widehat{a}_h(cm)$	$z_h(cm)$	$k_b(cm)$	$\widehat{a}_h/k_b$
211.0	8.4	282.33	100.0	2.27	124.0

Table 4: Parameters of Sleath's experimentation

Figures (1 and 2) compare the profiles of the velocity measured and simulated by $\overline{v'^2} - f$ and $q^2 - q^2\ell$ models. These comparisons are drawn during the acceleration and deceleration phases of the wave. From these figures one can observed that the profiles computed by the $\overline{v'^2} - f$ model are more consistent with the measurements than those performed by $q^2 - q^2\ell$ model. For the $\overline{v'^2} - f$ model, we find that the good agreement with measurements involves the totality of the water column, while for the $q^2 - q^2\ell$ model the relative consistency with the measures concerns only the bottom layer. This is probably due to the equilibrium assumption between production and dissipation of TKE used to derive the boundary conditions at the bottom for $q^2 - q^2\ell$ model. Figure (1) shows also that the model overestimates the BBL thickness.

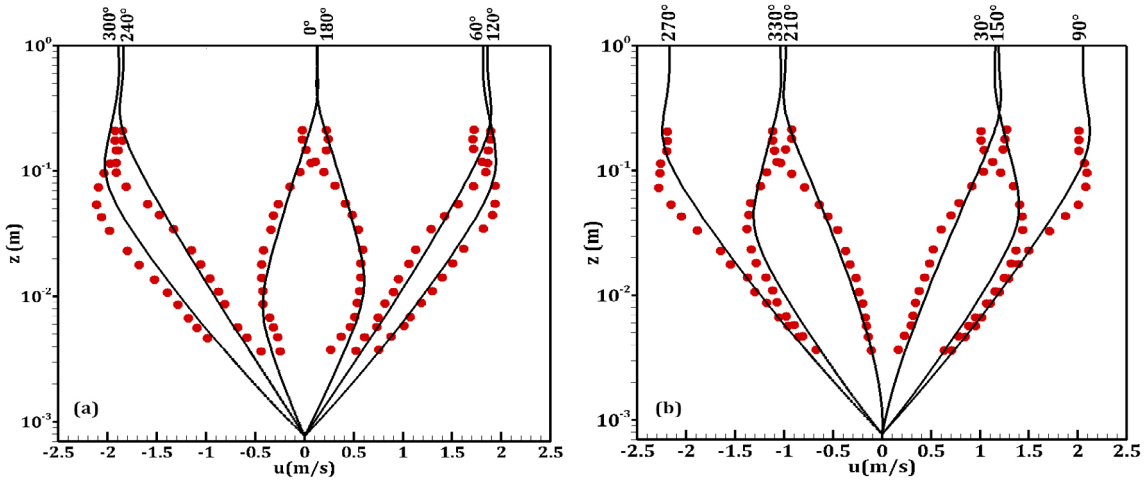

Figure 1: Comparison of velocity profiles: [•] measured; [-] computed by $q^2 - q^2\ell$. (a) acceleration phases; (b) deceleration phases

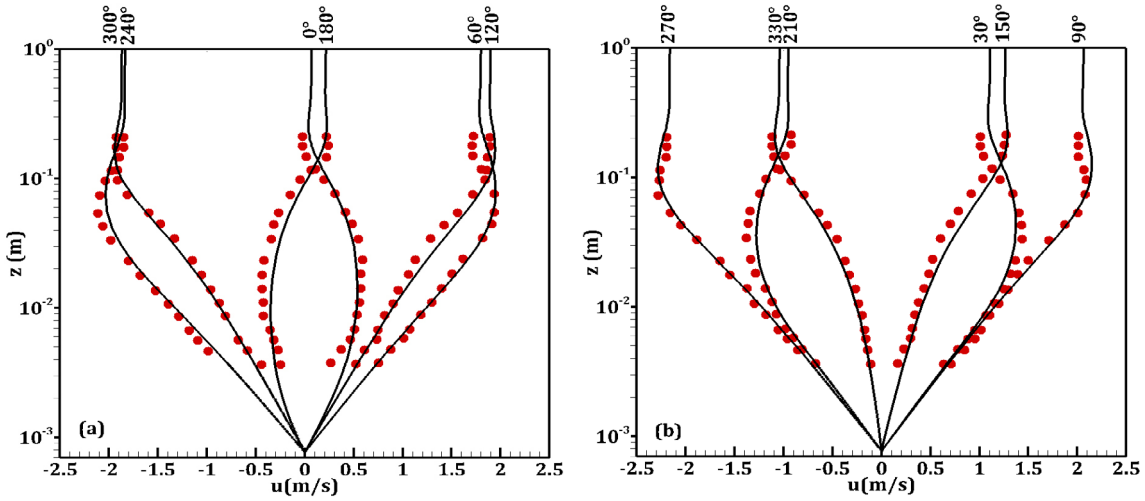

Figure 2: Comparison of velocity profiles: [•] measured; [-] computed by $\overline{v'^2} - f$. (a) acceleration phases; (b) deceleration phases

4 APPLICATION OF THE MODEL TO THE REAL CASE

4.1 Measurement area and measure instrumentation

Measurements used here were obtained at an shallow site located in the Eastern part of the English Channel. The measuring point is situated at one nautical mile of Hardelot beach at latitude $50°38.00'N$ and longitude $1°33.32'E$ in mean water depth of 16.5 m. The tidal period was semi-diurnal $T = 12.42h$. with a spring tide range of approximately $7m$.The bottom sediment at the Hardelot site is a silty sand with a median grain size of

$228mm$ comprising 11% silt and very fine sand, 48% fine sand, 28% medium sand, 5% coarse sand and 8%.
The instrumentation was deployed at the Hardelot site over the period 21-24 September 1997. The measurement platform is equipped with : ***(i)*** an Programmable Instrument (PI) resolving the inner bottom boundary layer, and ***(ii)*** an upward-looking $1200kHz$ Broad-Band Acoustic Doppler Current Profiler BBADCP scanning the outer bottom boundary layer. The PI incorporates a pressure sensor located at $2.17m$ above the bottom and four electromagnetic current meters measuring the horizontal velocities (u, v) at four desired heights. A series of water samples was collected every hour at $5m$ above the sea-bed during a tidal cycle. Total suspended sediment concentration values were obtained by filtration and plotted on semi-logarithmic graphs against the intensity of the BBADCP backscattered signals.
The tidal forcing of the 1DV-MoSeTT are provided by oscillating sea surface slopes (x-and y-direction) $(\frac{\partial \eta}{\partial x}, \frac{\partial \eta}{\partial y})$ related to the pressure gradient in the hydrodynamical quations (1) and (2). These quantities are derived from a two-dimensional vertically-integrated shallow-water model which covers the Eastern English Channel. The finite-difference model used is the MECCA model detailed in [11]. Let us note that the instrumentations deployed in the Hardelot site was measured pressure, horizontal velocity components (u, v) and the SPM. However, as the aim of this section is the test of the ability of the $\overline{v'^2} - f$ model to reproduce the SPM peaks observed in measurement area, we discuss only the results concerning the SPM. (for details on these measures see [12]).

4.2 Results and discussion

Predicted SPM concentration was performed for an available assemblage of 18 different classes of sediment reproducing distributions of natural sediment. The finest class taken into account is $45\mu m$. It should be noted that the amount of material in suspension depends on empirical parameter γ_0 (see equation 10). For the simulations carried out by the two models of turbulence, this parameter is taken equal to 3.2×10^{-3}. Figure (3) compares field measurements at $5m$ above sea bed with predictions of total SPM computed by the two models of turbulence. This figure shows that the two turbulence models reproduce the time variation in successive peaks influenced by asymmetry in tidal currents, as well as the variation associated with the neap-spring cycle. However, the $q^2 - q^2\ell$ model underestimates the maximum of the SPM. These differences with the measures are caused by the inability of this model to produce enough turbulence necessary to make bottom sediments in suspension. Disagreement is also observed during the reverses of neap periods characterized by low Reynolds number flow. However, the $q^2 - q^2\ell$ model has been designed specifically for the fully developed turbulence flow. It is therefore not surprising that this model fails at the neap periods.
Figure (3) clearly shows that the $\overline{v'^2} - f$ model remarkably improves the two anomalies produced by the $q^2 - q^2\ell$ model. We observe good agreement between the peaks of the

SPM produced by the $\overline{v'^2} - f$ model and those measured *in-situ*. From this figure, it can be deduced (as opposed to $q^2 - q^2\ell$ model) that the turbulence model $\overline{v'^2} - f$ produces sufficient turbulence to put the good quantity of sediments in suspension. This is probably due to the estimation of the turbulent viscosity ν_t as function of $\overline{v'^2}$ (instead of TKE) which takes into account the turbulence anisotropy near the bottom. Similarly, the $\overline{v'^2} - f$ model predicts correctly SPM minima including those corresponding to the neap tide when the flow is considered as low Reynolds number. This result is expected since the $\overline{v'^2} - f$ model is valid in the entire water column from bottom to surface without the damping functions.

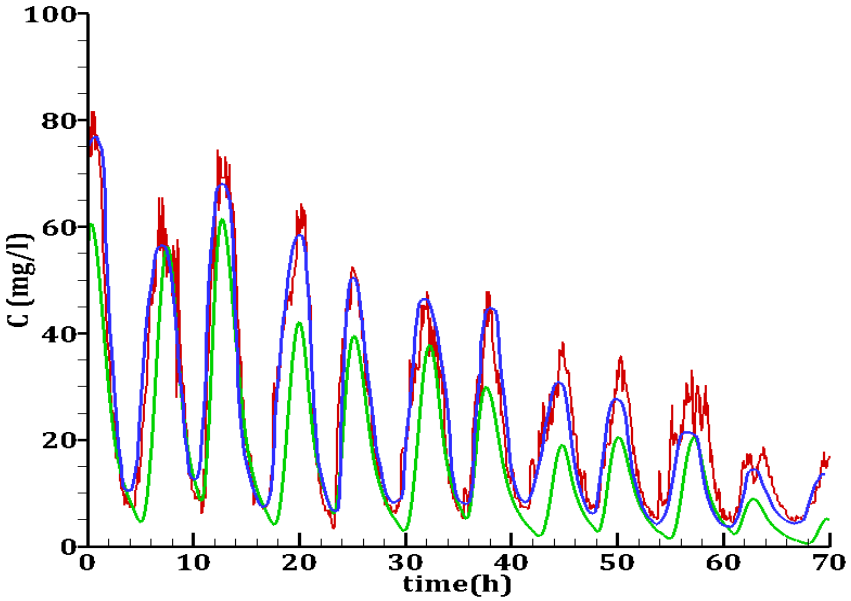

Figure 3: Time series of SPM at $5m$ above sea bed: red=measurements; green=computed by $q^2 - q^2\ell$; blue= computed by $\overline{v'^2} - f$

5 CONCLUSIONS

We have presented the 1DV-MoSeTT model for solving the sea bottom boundary layer and suspended sediment transport. Two turbulence models were implemented to compute the turbulent fluxes. Results of these two models were compared and confronted with laboratory and *in-situ* measurements to test their ability to reproduce the dynamics of suspended matter dynamics in the MBBL. From these comparisons, we deduce:

- The marked superiority of the $\overline{v'^2} - f$ model to reproduce the hydrodynamics.
- During the spring tide, the turbulent fluxes are correctly estimated by the model $\overline{v'^2} - f$ and consequently peaks and decreasing of suspension material are in good agreement with the *in-situ* measurements.

- During the reverses at the neap tide, $\overline{v'^2} - f$ model behaves as a low Reynolds number turbulence model. Consequently, SPM minima are fairly well reproduced.
- The $\overline{v'^2} - f$ model has the disadvantage of consuming more CPU time than the $q^2 - q^2\ell$ model, but with the 1DV version this disadvantage is not binding for computers with modest capacity (Intel Xeon CPU, 2.8 GHz, 8 cores, 16 GB of RAM).

REFERENCES

[1] Chien, K.Y. Predictions of channel and boundary-layer flows with a low-Reynolds number turbulence model. *AIAA Journal* (1982) **20**(1):33–38.

[2] Wilcox, D.C. Simulation of transition with a two-equation turbulence model. (1994) *AIAA Journal* **33**:247–255.

[3] Menter, F.R. Two-Equation Eddy-Viscosity Turbulence Models for Engineering Applications. (994) *AIAA Journal* **32**(8):1598–1605.

[4] Durbin, P.A. Near-wall turbulence closure modeling without damping functions. (1991) *Theoret. Comput. Fluid Dyn.* **3**:1–13.

[5] Mellor, G.L., and Yamada, T. Development of turbulence closure model for geophysical fluid problems. (1982) *Review of Geophysical Space Physics* **20**(4):851-875.

[6] Sleath, J.F.A. Turbulence oscillatory flow over rough beds. (1987) *J. Fluid Mech.* **182**:369–409.

[7] Van Rijn, L.C. *Principles of sediment transport in rivers, estuaries and coastal seas.* Amsterdam Aqua Publication 111, NUGI 186/831, (1993).

[8] Van Rijn, L.C. Sediment Transport, Part II: Suspended Load Transport. (1984) *J. Hyd. Engng.* **110**11:1613–1641.

[9] Durbin, P.A. A Reynolds stress model for near-wall turbulence. (1993) *J. Fluid Mech.* **249**:465–498.

[10] Davies, A.G., Soulsby, R.L., and King H.L. A numerical model of the combined wave and current bottom boundary layer. *J. Geophy. Res.* (1988) **93**(C1):491–508.

[11] Smaoui, H. and Radi, B. Comparative study of different advective schemes: Application to the MECCA model. *Env. Fluid Mech.* (2001) **1**(4):361–381.

[12] Smaoui, H., Boughanim, F. And Chapalain, G. 1D vertical model for suspended sediment transport in turbulent tidal flow: Application to the English Channel. *Compu. Geosci.* (2007) **33**:1111–1129.